

# Gcn5-mediated acetylation at MBF-regulated promoters induces the G1/S transcriptional wave

Alberto González-Medina, Elena Hidalgo and José Ayté\*

Oxidative Stress and Cell Cycle Group, Universitat Pompeu Fabra, Barcelona 08003, Spain

Received October 24, 2018; Revised June 17, 2019; Editorial Decision June 19, 2019; Accepted June 21, 2019

## ABSTRACT

In fission yeast, MBF-dependent transcription is inactivated at the end of S phase through a negative feedback loop that involves the co-repressors, Yox1 and Nrm1. Although this repression system is well known, the molecular mechanisms involved in MBF activation remain largely unknown. Compacted chromatin constitutes a barrier to activators accessing promoters. Here, we show that chromatin regulation plays a key role in activating MBF-dependent transcription. Gcn5, a part of the SAGA complex, binds to MBF-regulated promoters through the MBF co-activator Rep2 in a cell cycle-dependent manner and in a reverse correlation to the binding of the MBF co-repressors, Nrm1 or Yox1. We propose that the co-repressors function as physical barriers to SAGA recruitment onto MBF promoters. We also show that Gcn5 acetylates specific lysine residues on histone H3 in a cell cycle-regulated manner. Furthermore, either in a *gcn5* mutant or in a strain in which histone H3 is kept in an unacetylated form, MBF-dependent transcription is downregulated. In summary, Gcn5 is required for the full activation and correct timing of MBF-regulated gene transcription.

## INTRODUCTION

A conserved feature from yeast to human cells is the control of progression in the cell cycle, which is essential if cells want to continue proliferating appropriately (1). Key players involved in the cell cycle control are the cyclin-dependent kinases (CDKs) that, together with the different cyclins, phosphorylate hundreds of substrates that promote advancement through the different phases of the cell cycle (2). One of the key checkpoints of the cell cycle is placed at the end of the G1 phase, when there is the decision point between remaining in a state of quiescence (G0) or continuing the proliferative cycle. This point is known as Start in yeast and Restriction Point in mammalian cells (3). In the fission yeast *Schizosaccharomyces pombe*, the progression through Start depends on the activation of the transcription factor

MBF [Mlu cell-cycle box (MCB) Binding Factor], which is the functional homolog of E2F-RB in metazoans. MBF is a multimeric complex containing the essential core protein Cdc10 together with the DNA-binding proteins, Res1 and Res2 (4), and the co-activator, Rep2, whose function remains largely unknown (5). MBF mediates the G1/S specific transcription of <80 genes required for the completion of S phase (6–9). Canonical MBF targets include *cdc22* (ribonucleotide reductase) (10), *cig2* (S phase cyclin) (11), *cdc18* and *cdt1* (both are part of the DNA replication machinery) (12,13). Among the MBF-regulated genes, there are also some encoding proteins that are involved in a double negative feedback: whilst the cyclin Cig2 phosphorylates and inhibits MBF, Yox1 and Nrm1 bind the MBF complex at the end of S phase, switching off MBF-dependent transcription (14–18).

Deregulation of this transcriptional program results in replicative stress, which ultimately may induce DNA damage (19). Interestingly, when DNA replication is challenged, the checkpoint triggers an activation of the MBF-dependent transcription through inhibition of Yox1 (15). On the contrary, when the DNA damage checkpoint is activated, MBF-dependent transcription is downregulated through inactivation of Cdc10 (20). The pathways regulating both checkpoints and the G1/S transcriptional network converging in a single transcription factor to maintain the genome stability are highly conserved among eukaryotes (21,22). The importance of this interrelationship between the Restriction Point and the checkpoints for maintenance of the appropriate cell cycle control is confirmed by the high number of mutations that arise in the components of these pathways during oncogenesis (23,24).

The promoter architecture of genes is an important feature to activate gene expression under suitable conditions. Nucleosomes not only are useful in compacting the genome, but also regulate DNA-related processes like transcription, since they are an impediment to the union of the transcriptional machinery (25). The promoter architecture can be regulated by histone modifications, introducing post-translational covalent modifications to histones (26). These modifications impact transcription via two mechanisms: first, modulating the chromatin structure through alteration of the DNA–nucleosome interaction, allowing the entry of

\*To whom correspondence should be addressed. Tel: +34 933 160 847; Email: jose.ayte@upf.edu

the transcription machinery to the promoters (27); second, serving as an anchor for the binding of proteins with specialized domains such as bromodomains or chromodomains (28). Among all the histone modifications, acetylation has been widely correlated with gene activation. *Schizosaccharomyces pombe* has six acetyltransferases (HATs) involved in transcription regulation: Hat1, Mst1, Mst2, Gcn5, Rtt109 and Naa40. Gcn5 (General Control Non-derepressible 5) is a member of the GNAT family and the best-characterized HAT, serving as a prototype for histone acetyltransferase studies. Gcn5 is involved in the acetylation of histone H3 lysine 9 (H3K9), histone H3 lysine 14 (H3K14) and histone H3 lysine 18 (H3K18) (29), and has a bromodomain, allowing its binding to acetylated H3 and H4 tails and potentiating cooperative nucleosome acetylation of histone H3 (30,31). Gcn5 is a part of the conserved SAGA complex, a multifunctional co-activator that contains 19 proteins, and it is composed of five modules with diverse activities: structural core, transcription factor-binding module, histone acetyltransferase, histone deubiquitinase (DUB) and TATA-box binding protein (TBP) modules (32,33). The acetylation carried out by the HAT module allows the chromatin landscape to be opened up for binding of additional transcription factors and the pre-initiation complex (PIC) (34). Several SAGA subunits, including Spt3 and Spt8, collaborate (35) in the recruitment of TBP to facilitate PIC formation and transcriptional activation (35,36). Gcn5, together with SAGA, has been shown not only to be present at promoters, but also to localize to coding regions where they accompany Pol II during elongation and function to acetylate and evict nucleosomes from the gene coding regions (37,38). The DUB module promotes transcription elongation through deubiquitination of H2B, which allows recruitment of the Ctk1 kinase and subsequent Ser2 phosphorylation of the Pol II C-terminal domain (39).

The mechanisms by which regulators and DNA-binding transcription factors affect the recruitment and biological function of SAGA in the G1/S transcriptional wave are not fully understood. In mammalian cells, target genes bound by E2F1-3 show an increase in acetylated histones in late G1 phase, in parallel with activation of E2F-dependent transcription (40). While it has been shown that GCN5 interacted specifically with E2Fs stimulating its transcriptional activity (41), recent studies have shown that GCN5 acetylates H3K9 of almost all active genes in both budding yeast and mammalian cells (42). Additionally, E2F can also interact with KAT5, but the function of this HAT in E2F-regulated transcription is largely unknown (43). In parallel, some studies have shown that CBP, p300 and the P/CAF can acetylate E2F itself, increasing its DNA-binding ability and its transcriptional activation (44,45). Later works have shown that p300 and P/CAF can acetylate the repressor RB rather than E2F (46–49). Therefore, the specific role of HATs in the control of G1/S transcriptional program remains unknown.

This study was sought to elucidate the HATs regulating the G1/S transcriptional wave in *S. pombe*. We screened the recruitment of the different HATs to MBF-regulated promoters. Gcn5 turned out to be the main HAT to be recruited in an MBF-dependent manner through the co-activator Rep2. Gcn5 acetylated H3K9 and H3K18 at MBF

promoters during the G1/S transition, and this activity was required to maintain the full expression and proper timing of the G1/S transcriptional wave.

## MATERIALS AND METHODS

### Media, molecular genetics and growth conditions

All *S. pombe* strains are isogenic to wild-type 972 h- and are listed in Supplementary Table S1. Media were as described previously (50). Gene deletions or tagging were performed using a polymerase chain reaction (PCR)-based method (51). All deletions were confirmed by PCR on genomic DNA. Tagging was validated by western blotting. The histone H3 mutant strains were done as previously described (52). We cloned the entire *h3.2* locus by PCR from a wild-type strain. The PCR product was inserted into a Bluescript plasmid. We used two overlapping primers containing the mutated codons to amplify with primers annealing upstream or downstream of the gene. The product of this PCR was used as DNA template in a PCR in which the two external primers were used to amplify the entire *h3.2* histone gene. This PCR generated a mutated *h3.2* gene that was confirmed by sequencing and inserted into a plasmid. The mutated *h3.2* was amplified and used for transformation in a strain containing *h3.2::ura4+* (FY4754 from Robin Allshire lab). Positive colonies were selected using 5-FOA. The new strains were confirmed by PCR and sequencing. To determine the viability of each mutant, they were crossed with a strain harboring *h4.2::ura4 h3.1/h4.1Δ::his3+ h3.3/h4.3Δ::arg3+* (FY4640 from Robin Allshire lab). The final strains were confirmed by PCR and sequencing.

### Drug treatment

HU treatments were carried out on mid-log grown cultures ( $3-4 \times 10^6$  cells/ml) in YE5S media. To analyze sensitivity to DNA damage sources on plates, *S. pombe* strains were grown in liquid YE5S media to an OD<sub>600</sub> of 0.5. Cells were then diluted in YE5S and  $10-10^5$  cells per dot in a final volume of 3  $\mu$ l (using a replica plater) were spotted onto YE5S media agar plates containing (or not) HU. Plates were incubated at 30°C for 3–4 days.

### Cell synchronization

Cultures were synchronized at the end of G2 phase using the temperature-sensitive strain *cdc25-22* or at metaphase with *cdc2-asM17* strain. For *cdc25-22*, cells were cultured in minimal media at the permissive temperature (25°C) before shifting to non-permissive temperature (36°C) for 4 h and then released at permissive temperature. For *cdc2-asM17*, cells were cultured in minimal media and blocked using 1  $\mu$ M 1-NM-PP1 for 4 h, and then released by filtering the culture into fresh media. Synchronization in G1 phase was done by nitrogen starvation: log-phase cells were arrested using minimal medium lacking nitrogen for 16 h. Cells were released adding 2.5 mg/ml of NH<sub>4</sub>Cl, and samples were collected every hour. Samples from synchronizations were

analyzed on microscopy, FACS, RNA and/or ChIP experiments at the indicated time points. Septation index was measured from cell fixed in 70% ethanol and stained with 25  $\mu\text{g/ml}$  calcofluor.

### Flow cytometry

Cells were fixed on 70% ethanol. After washing with 50 mM of sodium citrate, cells were suspended in 50 mM sodium citrate containing RNase A (final concentration 0.2 mg/ml) at 37°C overnight. About 50 mM sodium citrate containing propidium iodide (final concentration 2.5  $\mu\text{g/ml}$ ) was added. Then cells were sonicated and the fluorescence intensities of stained cells was measured and analyzed on a FACSCalibur flow cytometer using CellQuest software. Twenty thousand events per sample were analyzed.

### Northern blot

Total RNA was extracted from 40 ml of cells at an  $\text{OD}_{600}$  of 0.5 by standard hot-phenol method, as described earlier (53). About 10  $\mu\text{g}$  of extracted RNA was loaded on formaldehyde agarose gels and transferred to membranes, which were hybridized with the [ $\alpha$ - $^{32}\text{P}$ ]-dCTP labeled *cdc18*, *cdc22* or *act1* probes, containing the complete ORFs.

### Reverse-transcription and quantitative (q)PCR

About 10  $\mu\text{g}$  of purified RNA were incubated with DNase I (Roche) for 30 min at 37°C, followed by purification using acid phenol–chloroform extraction. Reverse transcription was performed on 4  $\mu\text{g}$  of total RNA using Reverse Transcription System (Promega), as indicated in the manufacturer's manual. The cDNA was diluted 1:2 prior to PCR amplification. cDNAs were quantified by real-time qPCR on Light Cycler II using Light Cycler 480 SYBR Green I Master (Roche). The error bars (SEM) were calculated from at least three biological triplicates, unless indicated otherwise. Primers are listed in Supplementary Table S2.

### Protein analysis

Protein extracts were made by trichloroacetic acid (TCA) extraction and analyzed by western blotting as described previously (54). Antibodies used to detect proteins are listed in the Supplementary Table S3.

### Co-Immunoprecipitations

Co-immunoprecipitation analysis was carried out as previously described (55), with minor modifications. Cells from 100 ml cultures at an  $\text{OD}_{600}$  of 0.5 were pelleted and resuspended in lysis buffer (50 mM Tris-HCl, pH 7.5, 120 mM KCl, 5 mM EDTA, 0.5% NP-40 and 10% glycerol, 1 mM PMSF, 0.5 mM DTT, protease inhibitors cocktail) and lysed in a cryogenic grinder. Lysates were centrifuged and supernatants transferred to new microtubes. Rep2-TAP was immunoprecipitated from cleared supernatants by adding IgG Sepharose (GE Healthcare) for 2 h at 4°C. Immunoprecipitates were washed four times with lysis buffer. Proteins were released from immunocomplexes by boiling for

15 min in sodium dodecyl sulphate (SDS) loading buffer. Samples were separated by 8% SDS–polyacrylamide gel electrophoresis (PAGE) and detected by immunoblotting. Antibodies used to detect proteins are listed in the Supplementary Table S3.

### Chromatin immunoprecipitation (ChIP) assay

Chromatin immunoprecipitation (ChIP) assays were carried out as previously described (56) with minor modifications. Briefly, 50 ml of cells at an  $\text{OD}_{600}$  of 0.5 per sample were cross-linked adding 1% formaldehyde for 10 min for Gcn5-HA ChIPs and 20 min for all other proteins at 25°C; cross-linking was stopped with 125 mM glycine. Pellets were lysed with a bead beater in lysis buffer (50 mM HEPES–KOH, pH 7.5, 140 mM NaCl, 1 mM EDTA, 1% Triton X-100, 0.1% sodium deoxycholate, 0.1% SDS, 1 mM PMSF). Lysates were sonicated, yielding chromatin fragments of  $\approx 400$  bp average size. Chromatin lysate was immunoprecipitated with specific antibodies (see Supplementary Table S3) and protein G-Sepharose beads overnight at 4°C rotating. Beads were washed once in lysis buffer, twice in lysis buffer containing 0.5 M NaCl, twice in washing buffer (10 mM Tris, pH 8.0, 0.25 M LiCl, 0.5% NP-40, 0.5% sodium deoxycholate, 1 mM EDTA and 1 mM PMSF) and once in TE (10 mM Tris, pH 8.0, 1 mM EDTA). DNA was eluted by incubation of the beads for 20 min at 65°C with elution buffer (50 mM Tris, pH 7.5, 10 mM EDTA pH 8.0, 1% SDS), and further incubation in TE with 0.67% SDS. Formaldehyde cross-linking was reversed by overnight incubation at 65°C. Proteins were digested by incubation for 2 h at 37°C with 0.3 mg/ml proteinase K and 0.04 mg/ml glycogen. About 125 mM NaCl was added, chromatin was purified by phenol/chloroform extraction and precipitated with cold ethanol for at least 2 h at  $-20^\circ\text{C}$ . DNA was precipitated, air-dried and resuspended in TE buffer. Recovered DNA was amplified by quantitative real-time PCR using Light Cycler 480 SYBR Green I Master (Roche). The error bars (SEM) were calculated from at least three biological triplicates, unless indicated otherwise. The primers used are listed in Supplementary Table S2.

### Scatter plots

Scatter plots were generated using R software and ggplot2 package. The processed data from RNA microarrays were obtained from (57).

## RESULTS

### SAGA is recruited to MBF-regulated genes in a cell cycle and Rep2-dependent manner

To further elucidate the mechanism by which MBF was regulated, we decided to screen the binding of the different fission yeast histone acetyltransferases (HATs) to MBF-regulated promoters. We tagged each of the HATs with either HA or Myc in their native chromosomal locations and confirmed that these tags rendered strains that behaved like wild-type fission yeast in the presence of hydroxyurea (HU) (Supplementary Figure S1). These strains were used to test



their binding by ChIP to the promoter of the best characterized MBF-regulated genes, *cdc18* and *cdc22*. As can be observed in Figure 1A, Gcn5 and Rtt109 were the HATs that showed more binding to the promoters and also had increased recruitment after treatment with HU. It was previously described that an overall increased acetylation on H3K56 during S phase, mediated by Rtt109, was required to recover from replication stress (58,59). However, no major effect on H3K56 acetylation at MBF-regulated promoters was observed during an unperturbed cell cycle (see below), which prompted us to focus on the role of Gcn5. Since Gcn5 may be part of the SAGA or the ADA complexes, tests were carried out to ascertain whether Spt7, a core subunit of SAGA, could also bind to MBF-regulated genes. We observed that the recruitment of both Gcn5 and Spt7 after HU-treatment was mainly to the promoter region of the MBF-regulated genes (Figure 1B). Next, we wanted to determine whether Gcn5 was also recruited to MBF-regulated promoters during an unperturbed cell cycle, and not only under replicative stress conditions. To do so, we synchronized cells at the G2/M transition and then analyzed the binding of Gcn5 as cells progressed into the cell cycle. As can be observed in Figure 1C, Gcn5 was recruited to the promoters from M to S phase, coincident with the transcriptional activation of *cdc18* and *cdc22*.

To test whether the interaction between the MBF complex and the SAGA complex was direct, both complexes were co-immunoprecipitated. As bait, we decided to use the MBF co-activator, Rep2. As shown in Figure 2A, Gcn5 was specifically immunoprecipitated with Rep2 in a Tra1-dependent manner, confirming the interaction between the MBF complex (Rep2) and Gcn5. In fact, the recruitment of Gcn5 to promoters after HU treatment was abolished in strains in which either Rep2 or Tra1 was absent (Figure 2B). The fact that we could not detect an additive effect when both Rep2 and Tra1 were absent suggested that the interaction of both complexes was mediated through the interaction of Rep2 with Tra1. In fact, it was previously suggested that Tra1 was the SAGA complex protein that mediated the interaction with several transcription factors (32). Here, we showed that this interaction also required the MBF core protein Rep2 to occur. This Rep2-dependency was also shown in synchronized cultures: in the absence of Rep2 it was not possible to detect the cell cycle-regulated recruitment of SAGA to MBF-regulated promoters (Figure 2C and Supplementary Figure S2).

### The co-repressors, Nrm1 and Yox1, block the recruitment of SAGA

The previous experiments showed that the SAGA complex was recruited to MBF-regulated promoters through the co-activator Rep2. However, activation of MBF-dependent transcription can be achieved through the release of the co-repressor system Nrm1/Yox1, acting as a link between cell cycle and replicative stress with MBF-dependent transcription. To investigate whether Nrm1 and/or Yox1 also play a role in the recruitment of SAGA, we measured the recruitment of Gcn5 in strains deleted for *yox1* or *nrm1*. As shown in Figure 3A, in a  $\Delta yox1$  strain we detected full binding of Gcn5 even in the absence of HU treatment, when compared

to a wild-type strain. This binding was even increased in a  $\Delta nrm1$  strain, which correlated with the role of Nrm1 in bringing Yox1 onto the MBF complex.

To determine the epistatic relationship between the activator Rep2 and the co-repressors Nrm1 or Yox1, Gcn5 ChIPs were repeated comparing its recruitment in  $\Delta rep2$ ,  $\Delta nrm1$  and  $\Delta rep2 \Delta nrm1$  strains. As can be observed in Figure 3B, in the absence of both Rep2 and Nrm1 we could only detect a low level of Gcn5 recruitment onto MBF-regulated promoters, which was not enhanced after HU treatment. These results showed the essential role of Rep2 in Gcn5 recruitment to MBF-regulated promoters. In parallel experiments, we measured the expression of *cdc22* and *cdc18* (Figure 3C), which faithfully reflected the amount of Gcn5 that was recruited at the promoters. These results suggested that although the co-activator Rep2 mediated the recruitment of the SAGA complex onto MBF-regulated promoters, the co-repressors Nrm1 and/or Yox1 could act as a physical barrier to the loading of SAGA.

### Gcn5 acetylates H3K9 and H3K18 at MBF-regulated promoters

It has been described that Gcn5 was involved in the acetylation of at least three different residues in histone H3, lysines 9, 14 and 18, with some overlapping functions with another HAT, Mst2. We decided to determine which of these sites were acetylated at the MBF-regulated promoters. First, the specificity of the commercial antibodies -against each of these acetylated residues was tested on extracts prepared from wild-type,  $\Delta gcn5$ ,  $\Delta mst2$  and  $\Delta gcn5 \Delta mst2$  fission yeast strains. While Gcn5 was indeed involved in the acetylation of lysine 9, 14 and 18, Mst2 was only responsible for the partial acetylation of lysine 14 (Supplementary Figure S3A). Next, and as a first approach to determine which histone acetylation site was involved in the activation of MBF-regulated genes, we measured the H3K9, H3K14 and H3K18 acetylation at *cdc22* and *cdc18* genes, before and after HU treatment. As can be observed in Figure 4A, we detected an increase in the acetylation of these three residues after HU treatment. This increase was mainly observed in the promoter region of both genes. However, there were noticeable differences in the increase in acetylation among the three sites. While we detected a 3- or 4-fold increase for H3K9 and H3K18, respectively, we only detected a 1.5-fold for H3K14 (Figure 4B), indicating that after HU treatment, the main targets of acetylation were lysines 9 and 18, whose global acetylation was mainly dependent on Gcn5. To confirm this and to specifically check on MBF-regulated promoters, we tested H3K9, H3K14 and H3K18 acetylation comparing wild-type and  $\Delta gcn5$  strains, before and after treatment with HU (Figure 4C). As can be observed, Gcn5 was essential for the increase in the acetylation of H3K9 and H3K18 at MBF-regulated promoters after HU treatment. This leaves Mst2 as, probably, the main HAT involved in the H3K14 acetylation. Similarly, and as expected, Rep2 was also required to increase H3K9 and H3K18 acetylation at *cdc18* and *cdc22* promoters (Supplementary Figure S3B).

To confirm that the acetylation of H3K9 and H3K18 at MBF-regulated promoters was transcription and cell cycle-

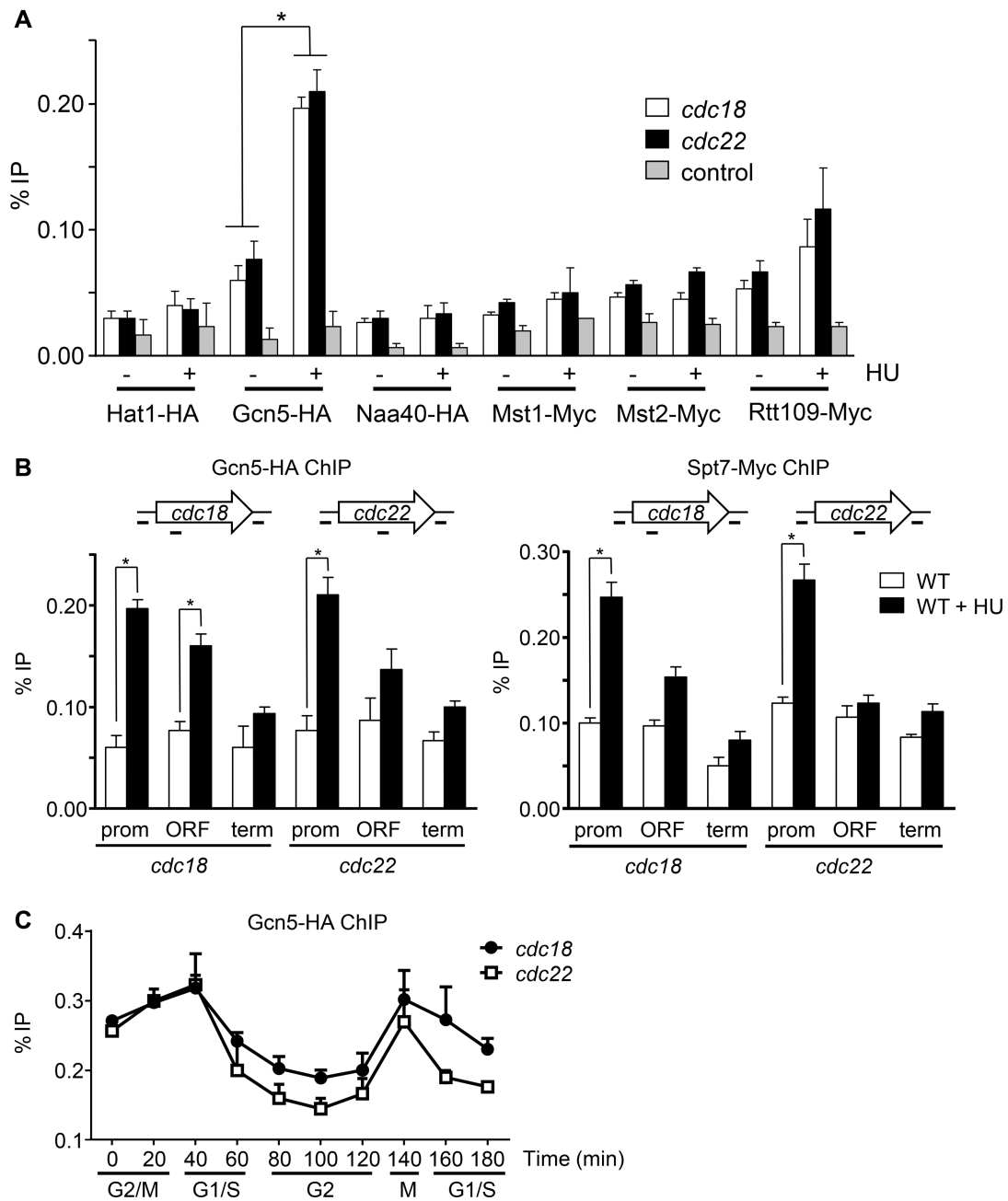


**Figure 1.** Gcn5 is recruited to MBF-regulated promoters. (A) Cells expressing the different HATs tagged with HA or Myc were treated (+) or not (–) with 12mM HU for 3 h. Binding of the HATs was determined by ChIP to the MBF-dependent promoters *cdc18* and *cdc22*. Primers from an intergenic region were used as negative control (control). Error bars (SEM) were calculated from biological triplicates and significant differences were determined by the Student’s *t*-test (\**P* < 0.05). (B) Cells expressing Gcn5-HA (left panel) or Spt7-Myc (right panel) were treated (+) or not (–) with HU for 3 h. ChIP experiments were performed using primers covering promoter (prom), coding (ORF) and termination (term) sequences of the *cdc18* and *cdc22* genes (as shown on top). Error bars (SEM) were calculated from biological triplicates. Significant differences between treated and untreated samples were determined by the Student’s *t*-test (\**P* < 0.05). (C) Fission yeast *cdc25.22 gcn5-HA* cells were synchronized at the G2/M transition. After release, samples were collected every 20 min and processed for ChIP against Gcn5-HA. Error bars (SEM) were calculated from biological triplicates. The different phases of the cell cycle are indicated at the bottom.

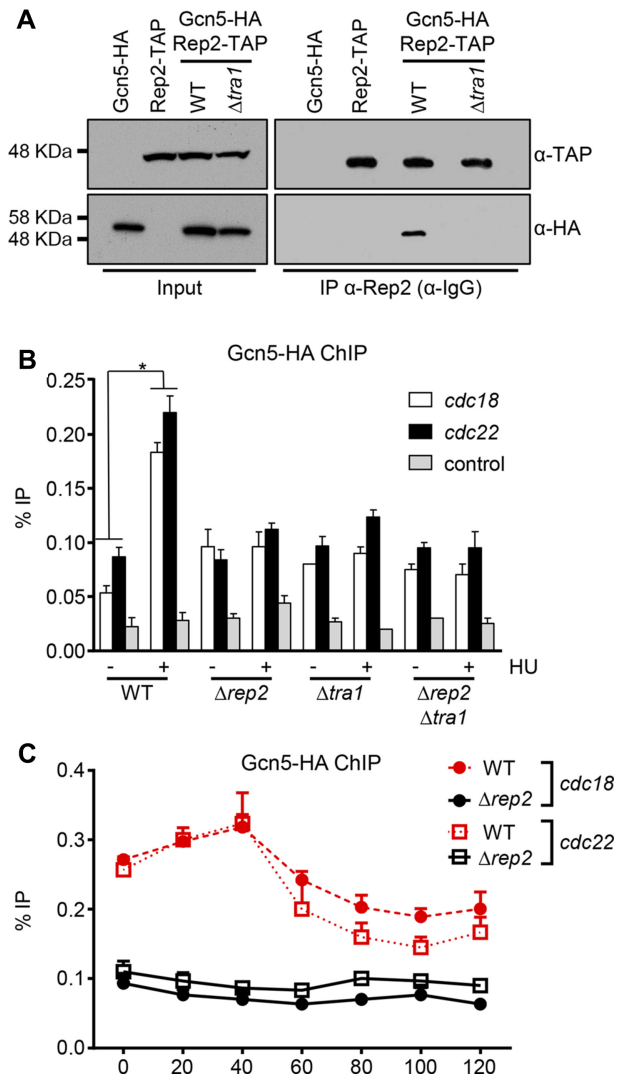


**Figure 2.** Rep2 recruits Gcn5 to MBF-regulated promoters in a Tra1-dependent manner. (A) Extracts prepared from cells expressing Gcn5-HA and/or Rep2-TAP were immunoprecipitated with IgG-sepharose (IP  $\alpha$ -TAP). Precipitated proteins were detected by Western Blot  $\alpha$ -TAP or  $\alpha$ -HA (right). Input is shown at the left. (B) Wild type (WT),  $\Delta rep2$ ,  $\Delta tra1$  and  $\Delta rep2 \Delta tra1$  cells expressing Gcn5-HA were treated (+) or not (-) with 12mM HU for 3 hours. Binding of Gcn5 to MBF-regulated promoters in these strains was determined by ChIP, as described. Significant differences before and after HU treatment were determined by the Student's t-test (\* $P < 0.05$ ). (C) Cultures of *cdc25.22 gcn5-HA* (red) *cdc25.22  $\Delta rep2 gcn5-HA$*  (black) cells were synchronized at the G2/M transition. Samples were collected every twenty minutes and processed for Gcn5 ChIP onto *cdc18* or *cdc22* promoters.

dependent and not an effect of the treatment with HU, we measured the H3K9, H3K14 and H3K18 acetylation on synchronized cultures comparing cells at the G1/S transition (when MBF-dependent transcription was fully induced) with cells in G2 (when MBF-dependent transcription was repressed). A noticeable increase could be observed in the acetylation of H3K9 and H3K18 concomitant with the activation of *cdc22* and *cdc18* transcription (Figure 4D) and a concomitant eviction of total histone H3, which was dependent on Rep2, Yox1, Nrm1 (Supplementary Fig-

ure S4A) and Gcn5 in synchronized cultures (Supplementary Figure S4B). However, no changes were observed in the acetylation level of H3K14 in the synchronous cultures (Figure 4D). Overall, these results showed that the acetylation changes that we observed in H3K14 after HU treatment most probably reflected the activation of the checkpoint caused by HU treatment and not an effect of transcription, as proposed previously (60). Furthermore, these changes in H3K14 acetylation were not caused by Gcn5.

H3K56 acetylation is another histone modification that could also be involved in the regulation of the G1/S transcriptional wave, since it was described to be increased in total extracts during S phase via the activity of Rtt109. We already showed that Rtt109 was recruited to some extent at MBF-regulated promoters after HU treatment (Figure 1A). When we measured H3K56 acetylation after HU treatment, we observed increased levels of acetylation throughout gene body of *cdc18* and *cdc22* and, specifically, to the promoter and terminator region of both genes (Supplementary Figure S5A), which reflected previous genome-wide observations (61). However, the fact that we did not detect changes in the H3K56 acetylation in synchronized cultures (Supplementary Figure S5B) and that *cdc18* or *cdc22* transcription was barely affected in  $\Delta rtt109$  cells (Supplementary Figure S5DE), led to the conclusion that this H3 modification did not have a major role in the normal regulation of the MBF-dependent genes, although it may have a minor role after HU treatment. Also, it is worth noting that we could detect a constitutive although partial Chk1 phosphorylation in  $\Delta rtt109$  cells (Supplementary Figure S5F), which indicated that the DNA damage checkpoint was activated in this background. In consequence, the minimal effect on transcription that we detected in  $\Delta rtt109$  cells could be caused through Chk1 activation: it was previously reported that MBF-dependent transcription is reduced when Chk1 is activated (20).

### SAGA is required for the correct timing of MBF induction

It has been previously shown that SAGA was involved in the activation of transcription of a majority of genes in many organisms, including fission yeast (32). We analyzed the effect that the deletion of each viable SAGA component ( $\Delta tra1$ ,  $\Delta gcn5$ ,  $\Delta ada2$ ,  $\Delta ada3$ ,  $\Delta sgf29$ ,  $\Delta ubp8$ ,  $\Delta sgf11$ ,  $\Delta sgf73$ ,  $\Delta sus1$ ,  $\Delta ada1$ ,  $\Delta spt7$ ,  $\Delta spt20$  or  $\Delta spt8$ ) has on the 15 best characterized MBF-regulated genes. As can be observed in Supplementary Figure S6A, the deletion of genes from either the structural core or the transcription factor-binding modules decreased, to some extent, the transcription of most of the analyzed MBF-regulated genes. To obtain a better view of the effect of the mutants, we represented a scatter plot of all gene expression changes, comparing  $\Delta tra1$ /WT versus  $\Delta gcn5$ /WT (Figure 5A),  $\Delta ada2$ /WT versus  $\Delta gcn5$ /WT and  $\Delta spt7$ /WT versus  $\Delta gcn5$ /WT datasets (Supplementary Figure S6B and C). The expression of the MBF-regulated genes, which are shown in red, is down-regulated when compared with the fission yeast transcriptome, indicating a specific effect of SAGA on the regulation of MBF-dependent genes.

Next, we decided to characterize the effect on *cdc22* and *cdc18* expression, comparing a wild-type strain with

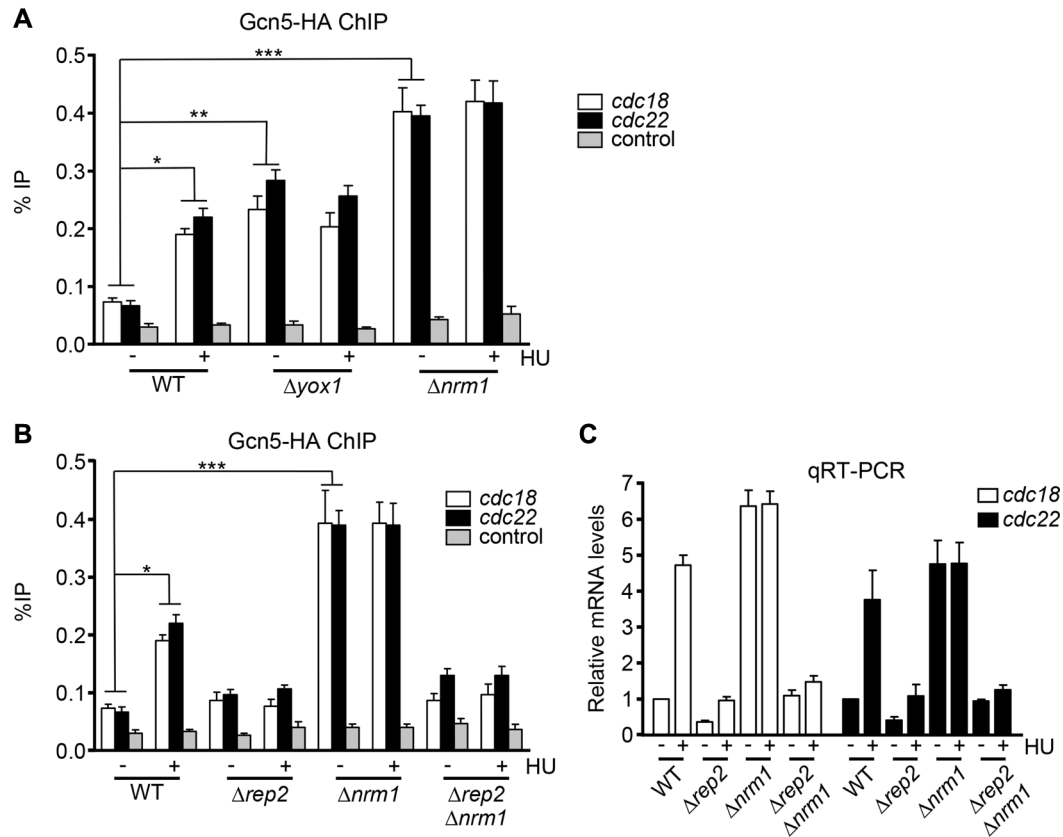


**Figure 3.** The co-repressors, Nrm1 and Yox1, are barriers for Gcn5 recruitment. (A) Wild-type (WT),  $\Delta yox1$  or  $\Delta nrm1$  cells expressing Gcn5-HA were treated (+) or not (-) with 12mM HU for 3 h. Gcn5 binding to *cdc18* or *cdc22* promoters was measured by ChIP as described before. Error bars (SEM) were calculated from biological triplicates. Significant differences were determined by the Student's *t*-test (\* $P < 0.05$ ; \*\* $P < 0.01$ ; \*\*\* $P < 0.001$ ). (B) Wild-type (WT),  $\Delta rep2$ ,  $\Delta nrm1$  and  $\Delta rep2 \Delta nrm1$  cells expressing Gcn5-HA were treated (+) or not (-) with HU for 3 h. Gcn5 binding to *cdc18* or *cdc22* promoters was measured by ChIP. Error bars (SEM) were calculated from biological triplicates. Significant differences were determined by the Student's *t*-test (\* $P < 0.05$ ). (C) Expression of the MBF-dependent genes *cdc18* and *cdc22* were analyzed by RT-qPCR in the indicated strains, before (-) and after (+) treatment with HU for 3 h. *tfb2* was used as a control for normalization. Each column represents the mean value and SEM, calculated from three biological replicates.

$\Delta rep2$ ,  $\Delta nrm1$  (which would give the minimum and the maximum expected, respectively),  $\Delta gcn5$  and  $\Delta nrm1 \Delta gcn5$  strains (Figure 5B). Whilst the effect on *cdc22* and *cdc18* expression caused by the deletion of *gcn5* could be confirmed, the effect was more noticeable when the transcription of these genes was constitutively induced (compare  $\Delta nrm1$  with  $\Delta nrm1 \Delta gcn5$  strains). Next, the expression of *cdc22* and *cdc18* in synchronous cultures released from a G2/M arrest was measured (Supplementary Figure S7A and B). As can be observed, the expression of *cdc22* and *cdc18* was decreased and slightly delayed in  $\Delta gcn5$  cells. The analysis was extended to other MBF-regulated genes, with the same effect being observed (Figure 5C,D and Supplementary Figure S7C), although it was more noticeable in those that are early induced genes, like *cdc18* and *cdt1*, than in those belonging to the late-induced genes, like *cdc22*, *cdt2*, *ssb1* and *yox1*.

The results shown above showed that Gcn5 (and SAGA) was involved in the acetylation of histones in the promoters of MBF-regulated genes and, in consequence, could have an important role in the G1/S wave of transcriptional activation. To confirm that Gcn5 was indeed acetylating histones at MBF promoters, we generated mutants in H3K9 and/or

H3K18 to prevent their acetylation (Figure 6A). Interestingly, all mutants exhibited sensitivity to HU, with the double mutant H3K9RK18R showing a similar phenotype to the  $\Delta gcn5$  strain (Figure 6B). As a first approximation, we measured *cdc22* and *cdc18* expression in these strains, comparing the asynchronous level to HU-treated cells. As can be observed in Figure 6C, the mutations (especially the double mutant, H3K9RK18R) moderately, but consistently, tapered down the expression of *cdc18* and *cdc22*. Next, we measured the effect of the histone mutations on synchronous cultures. First, we introduced the two single H3 mutants and the double mutant in a *cdc25-22* background, which would allow the arrest of the cells at the G2/M transition followed by synchronous release of the cultures. Unfortunately, these mutations in this genetic background did not allow for synchronization, since the cells were not properly released from the G2/M arrest. We decided then to use alternative systems to obtain synchronous cultures of these strains. First, we introduced the histone mutants in a *cdc2-asM17* background, which allows the synchronization of the cultures in metaphase (62). Both the *cdc2-asM17* strain and the *cdc2-asM17 H3K9RK18R* strain progressed with similar synchronicity with the septation peak after 60

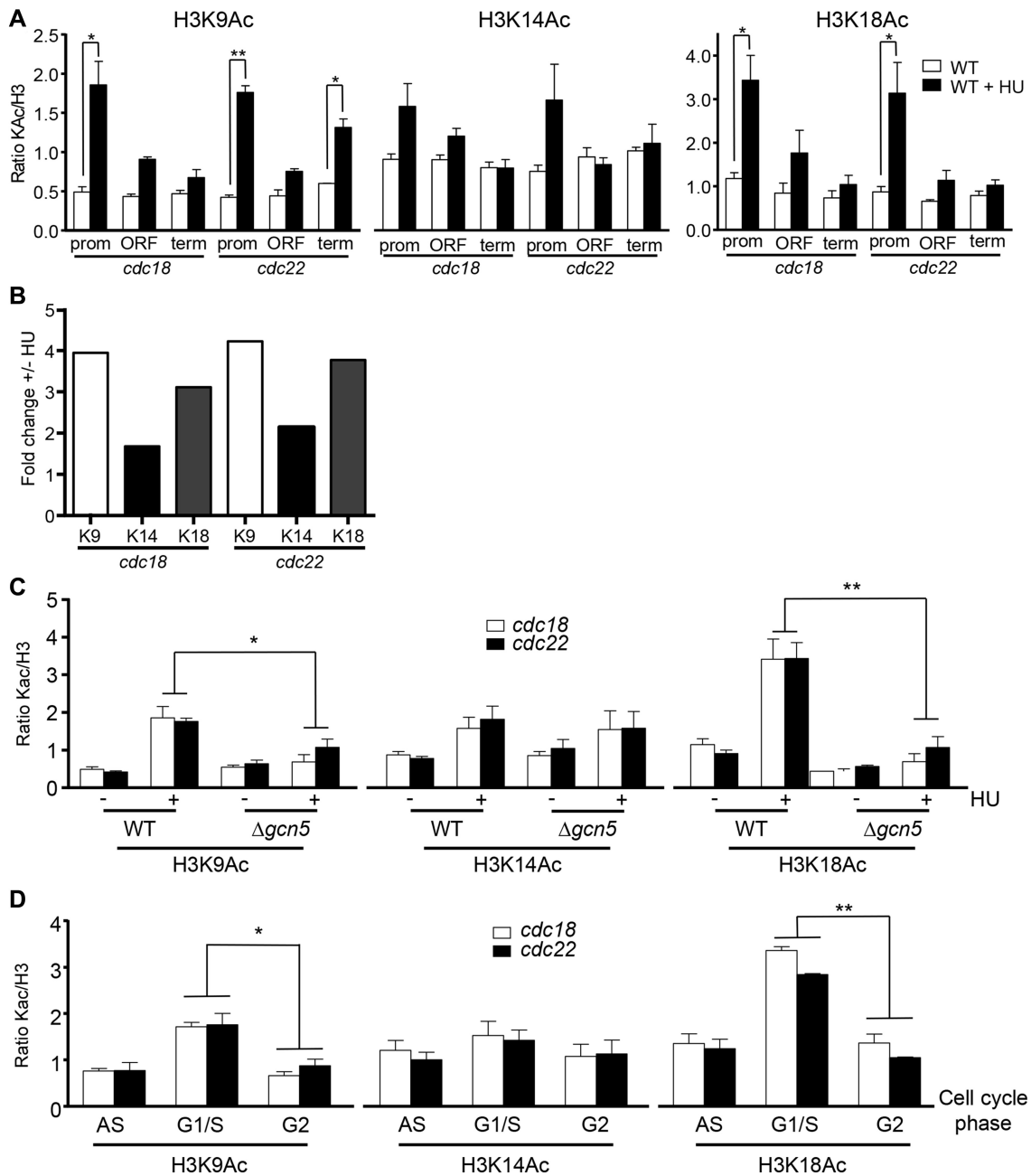


**Figure 4.** Histone H3 is acetylated at MBF promoters. (A and B) Cells treated (+) or not (–) with HU for 3 h were processed for ChIP against total histone H3, H3K9ac, H3K14ac and H3K18ac using primers covering promoter (prom), coding (ORF) and termination (term) sequences of the *cdc18* and *cdc22* genes. H3ac/H3 average ratios and SEM were calculated from three biological replicates. Significant differences were determined by the Student's *t*-test ( $*P < 0.05$ ;  $**P < 0.01$ ). Ratio of each H3 acetylation of treated versus untreated was calculated for promoters (B). (C) Wild-type and *gcn5* mutant cells were treated (+) or not (–) with 12mM HU for 3 h and processed for ChIP to determine the ratio of acetylated K9, K14 and K18 in the promoters, as described in panel (A). H3ac/H3 average ratios and SEM calculated from three biological replicates are shown. Significant differences were determined by the Student's *t*-test ( $*P < 0.05$ ;  $**P < 0.01$ ). (D) *cdc25-22* cells were released from a G2/M arrest, samples were collected at 40 min (G1/S) and 100 min (G2) and processed together with a sample from an asynchronous culture (AS) for ChIP to determine acetylated residues on the indicated promoters. H3ac/H3 ratios and SEM were calculated from biological triplicates. Significant differences were determined by the Student's *t*-test ( $*P < 0.05$ ;  $**P < 0.01$ ).



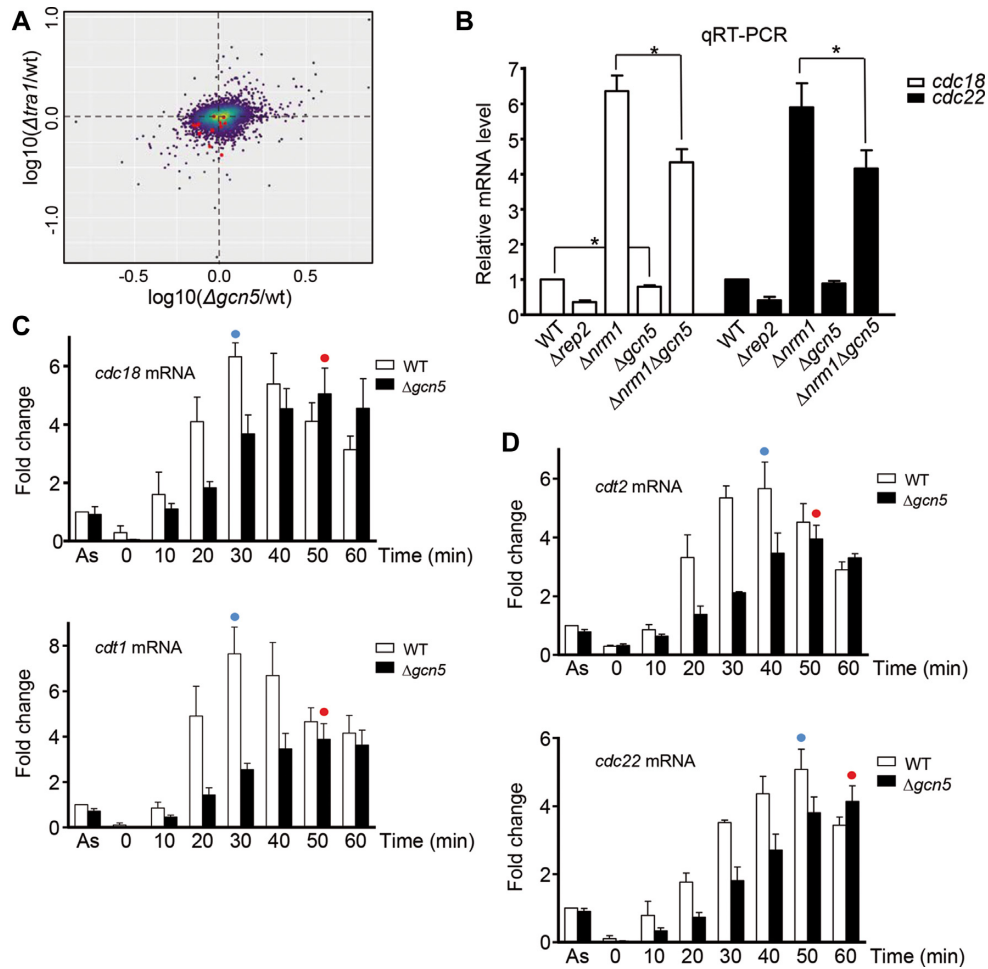


**Figure 5.** Gcn5 is required for the full activation of MBF-dependent transcription. (A) Scatter plots comparing the genome wide transcriptome available data (32) of *gcn5* and *tra1* mutant cells. The mRNA level of each mutant is relative to the levels of wild-type cells. Dots represent each of 3502 analyzed genes. The color of these dots represents the density of the points (less dense, purple, denser, yellow). Red dots represent the best characterized 15 MBF-dependent genes. The scale of both axes is  $\log_{10}$ . (B) Expression of *cdc18* and *cdc22* was analyzed by RT-qPCR in the indicated strains and compared to the wild-type (WT). *tfb2* was used as a control for normalization. Each column represents the mean value and SEM, calculated from three biological replicates. Significant differences were determined by the Student's *t*-test ( $*P < 0.05$ ). (C and D) Expression of early (C) or late (D) MBF-dependent genes was analyzed in *cdc25-22* and  $\Delta gcn5$  *cdc25-22* cells by RT-qPCR. Cells were synchronized at G2/M and after release samples were collected at the indicated times. *tfb2* was used as a control for normalization. Values from asynchronous cultures (As) of *cdc25-22* cells were set to 1 to allow comparisons across time and strains. Each column represents the mean value and SEM calculated from at least three biological replicates. The peaks of expression in *cdc25-22* and *cdc25-22*  $\Delta gcn5$  are marked by a blue/red dot, respectively.

min of the release (Supplementary Figure S8A). We isolated RNA as cells progressed into G1 and S phases and measured the level of *cdc22*, *cdc18*, *cdt1* and *cdt2* mRNAs. As shown in Figure 6D, the expression of all the MBF genes that were tested was reduced in the *H3K9RK18R* strain when cells entered into G1 phase, compared to the wild-type strain. Interestingly, in this genetic background (*cdc2-asM17*), we did not observe decreased expression in the asynchronous cultures. To confirm that acetylation of histone H3 at lysines 9 and 18 was indeed required to achieve full induction of the MBF-regulated genes independently of the genetic background, we analyzed the expression of MBF-regulated genes in a wild-type background as they re-entered in G1 phase from a nitrogen starvation. While both strains, wild-type and *H3K9RK18R*, entered from G0 into S phase at roughly the same time (3 h after placed in fresh media) (Supplementary Figure S8B), the expression of

the MBF-dependent genes was reduced in the *H3K9RK18R* cells, when compared to the wild-type cells ( $\Delta h3.1 \Delta h3.3$ ) (Supplementary Figure S8C), confirming the observation in the *cdc2-asM17* cells.

## DISCUSSION

Diverse nuclear molecular processes can be regulated through different levels of DNA packaging. Among them, transcription is one of the processes that is more tightly dependent on the level of chromatin compaction. Here, we propose that the HAT Gcn5 is required to fully activate the G1/S transcriptional wave through regulation of the MBF complex (Figure 7). This is achieved by active recruitment of the SAGA complex by the MBF co-activator and core element Rep2: the interaction between Rep2 and Tra1 (which is part of the SAGA complex) is responsible for bringing the

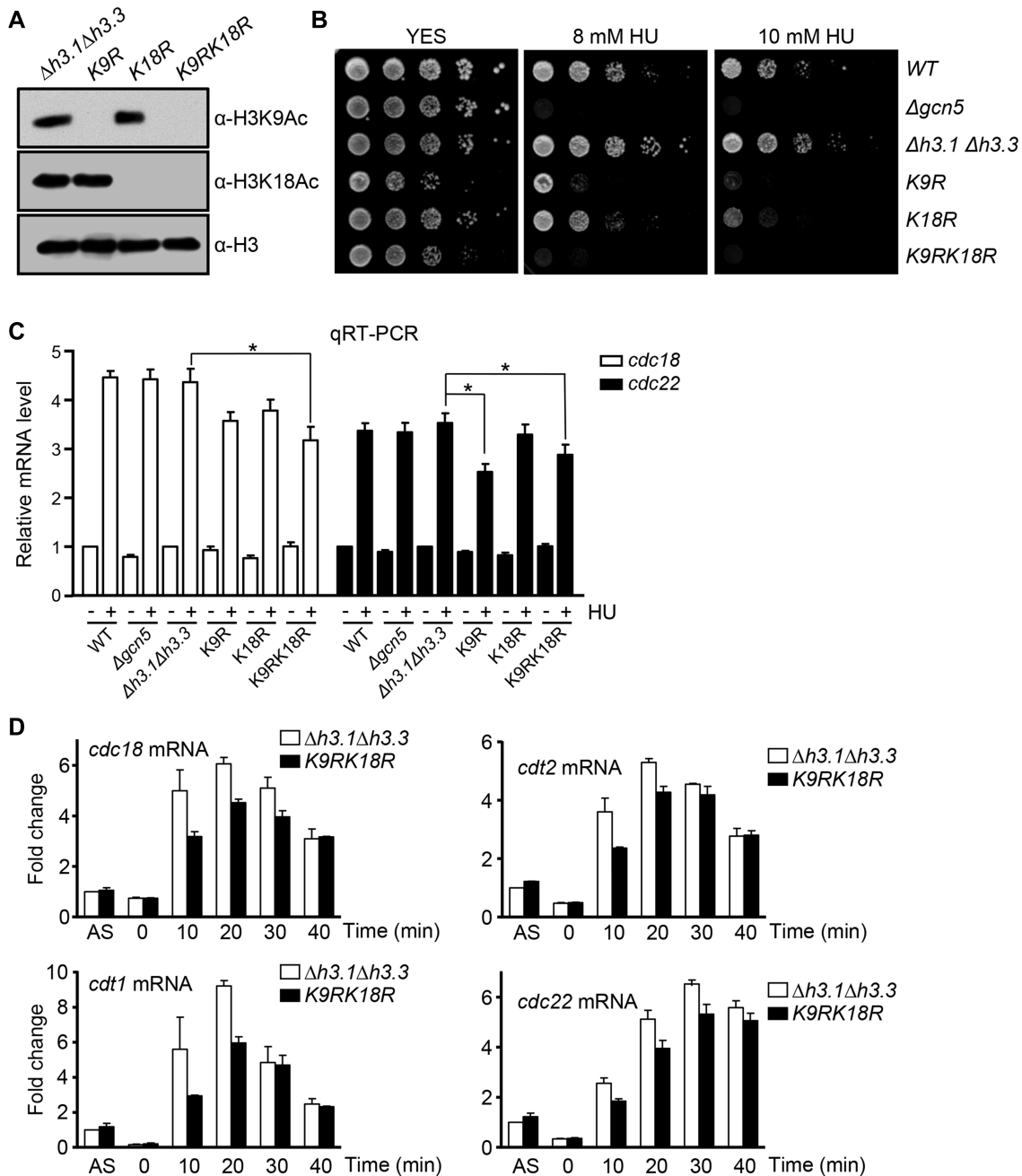


**Figure 6.** Acetylation of H3K9 and H3K18 is important to maintain full activation of MBF-dependent genes. (A) Extracts prepared from wild-type ( $\Delta h3.1\Delta h3.3$ ) and the histone H3 mutants H3K9R (K9R), H3K18R (K18R) and H3K9RK18R (K9RK18R) were analyzed with the antibodies indicated on the right. Total histone H3 ( $\alpha$ -H3) was used as a control. (B) Five-fold serial dilutions of the fission yeast strains indicated on the right were spotted onto rich media (YES) or in media with 6 or 8 mM HU. Plates were incubated at 30°C for 2–4 days. (C) Expression of *cdc18* and *cdc22* was analyzed by RT-qPCR in the indicated strains treated (+) or not (–) with HU for 3 h. *tfb2* was used as a control for normalization. Normalized mRNA levels in the untreated wild-type (WT) and in the parental strain for the H3 mutants ( $\Delta h3.1\Delta h3.3$ ) were set to 1 to allow comparisons across different strains. Each column represents the mean value and SEM calculated from four biological replicates. Significant differences were determined by the Student's *t*-test ( $*P < 0.05$ ). (D) Expression of *cdc18*, *cdt1*, *cdt2* and *cdc22* was analyzed in *cdc2-asM17* and *cdc2-asM17*  $\Delta gcn5$  cells by RT-qPCR. Cells were arrested at metaphase with 1  $\mu$ M 1-NM-PP1 inhibitor and after release, samples were collected at indicated times. *tfb2* was used as a control for normalization. Normalized levels in asynchronous (AS) *cdc2-asM17* strain were set at 1 to allow comparisons across time and strains. Each column represents the mean value and SEM calculated from at least three biological replicates.

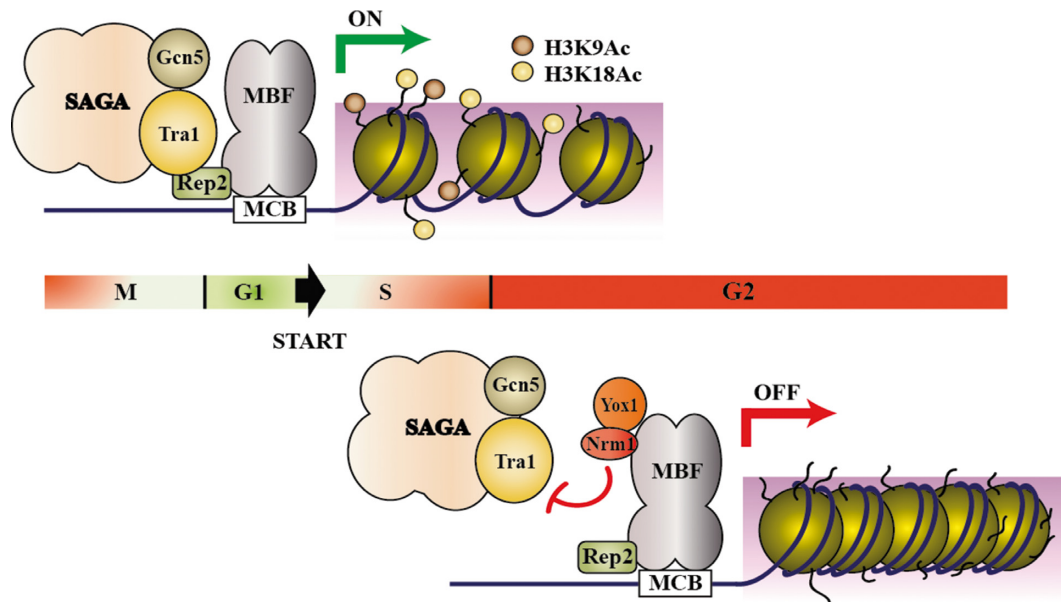


**Figure 7.** Model of SAGA and Gcn5 regulation of MBF-dependent genes. During Mitosis, SAGA complex binds to MBF complex through the interaction of the recruitment module Tra1 with the co-activator Rep2. Gcn5 acetylates specifically H3K9 and H3K18 within MBF promoters, leading to expression of G1/S transcriptional wave. But at the end of S phase, the co-repressors Nrm1 and Yox1, which are MBF targets genes, binds to MBF and blocks the recruitment of SAGA complex, turning off the MBF-dependent transcription. Although not shown here, we do not exclude other activators/repressors or other histone modifications as being equally responsible for the regulation of MBF-dependent transcription.

HAT activity to MBF-regulated promoters. In fact, this is the first time that the mechanism by which Rep2 manages to activate the transcription of MBF-regulated genes has been described. The HAT activity at MBF-regulated promoters is cell cycle-regulated, with its peak activity during the G1 and S phases of the cell cycle, which parallels a reduction in the total amount of histone H3 at these promoters. Interestingly, Gcn5 recruitment, rather than being positively regulated through a yet undisclosed regulation, seems to be only negatively regulated by the repressors of MBF activity, Nrm1 and Yox1. We have shown that Nrm1 (and Yox1, although to a lesser extent) interferes in the interaction between the MBF complex and the SAGA complex. In fact, in  $\Delta nrm1$  or  $\Delta yox1$  cells, Gcn5 binds constitutively to the MBF complex. The consequence of having a negative regulator dominant over a positive activator is that the MBF complex is always committed to inducing transcription, but inhibited when bound by Nrm1/Yox1. Somehow, this is reminiscent of how G1/S transcriptional wave is regulated in metazoans: the repression of hypophosphorylated pRB on E2F/DP1 is dominant over the transcriptional activators that are brought by E2F/DP1. Our findings also provide evidence supporting the hypothesis that the inhibition of MBF-dependent transcription happens as a consequence of the absence of positive regulators rather than an active mechanism required to stabilize repression.

Gcn5 is specifically brought to MBF-regulated promoters causing the acetylation of histone H3 at K9 and K18 residues. This acetylation is ultimately responsible for the transcription activation of the MBF-regulated genes at the G1/S transition. In the absence of Gcn5 or the timely acetylation of histone H3 at MBF-regulated promoters, cells are more sensitive to challenges to DNA synthesis. Thus, his-

tone H3 mutants that cannot be acetylated at lysines 9 and 18 recapitulate the transcription profile observed in  $\Delta gcn5$  cells in regard to MBF-dependent regulation. This does not imply that H3K9 and H3K18 are the unique acetylations that take place in MBF-regulated genes. We have shown that H3K14 is also acetylated by a different HAT, but only under replicative stress (Figure 4), which is when Mst2 has its major role (60). We have also shown that there is some acetylation on MBF-regulated genes at H3K56. In global genome studies, this acetylation, which was shown to be done by Rtt109, takes place during S phase and it is necessary to recover from DNA damage (59); and like the H3K14 acetylation, it is also related to replicative stress. However, we have shown that none of them take place under normal cell cycle progression in synchronous cultures. Finally, there is a fourth HAT, Mst1, that could be regulating MBF-dependent transcription, although through a very different mechanism. It has been described that Mst1 can acetylate the histone variant H2A.Z (Pht1 in fission yeast) (63). We have recently shown that H2A.Z acetylation affects the size of the Nucleosome Depleted Region (NDR); in the absence of H2A.Z acetylation, the NDRs preceding MBF genes decrease in size and transcription of MBF-regulated genes is downregulated (64). Thus, histone acetylations on other sites cannot be ruled out, but we propose that acetylations on H3K9 and H3K18 are the main targets to activate the G1/S transcriptional wave. Further experiments to check the recruitment of other chromatin modifiers in the absence of Gcn5 or in the H3K9RK18R mutant are required to determine if the acetylation in these two sites is essential to recruit other chromatin regulatory proteins, and to understand how the signal is transduced to achieve the transcriptional induction of this group of genes.

**SUPPLEMENTARY DATA**

Supplementary Data are available at NAR Online.

**ACKNOWLEDGEMENTS**

We thank Robin Allshire, Dom Helmlinger and Masamitsu Sato for providing strains. We thank members of the Oxidative Stress and Cell Cycle Group for suggestions and comments, David Castillo for the informatics analysis and Mercè Carmona for technical support.

**FUNDING**

Spanish Ministerio de Economía y Competitividad, PLAN E, and Feder [BFU2015-66347, PGC2018-097248-B-I00]; MEIONet [BFU2015-71786-REDT]; Unidad de Excelencia Maria de Maeztu [MDM-2014-0370]; ICREA Academia Award (Generalitat de Catalunya) (to E.H.). Funding for open access charge: Spanish Ministerio de Economía y Competitividad [BFU2015-66347, PGC2018-097248-B-I00].

*Conflict of interest statement.* None declared.

**REFERENCES**

- Bertoli, C., Skotheim, J.M. and de Bruin, R.A. (2013) Control of cell cycle transcription during G1 and S phases. *Nat. Rev. Mol. Cell Biol.*, **14**, 518–528.
- Coudreuse, D. and Nurse, P. (2010) Driving the cell cycle with a minimal CDK control network. *Nature*, **468**, 1074–1079.
- Pardee, A.B. (1989) G1 events and regulation of cell proliferation. *Science*, **246**, 603–608.
- Ayte, J., Leis, J.F., Herrera, A., Tang, E., Yang, H. and DeCaprio, J.A. (1995) The Schizosaccharomyces pombe MBF complex requires heterodimerization for entry into S phase. *Mol. Cell Biol.*, **15**, 2589–2599.
- Nakashima, N., Tanaka, K., Sturm, S. and Okayama, H. (1995) Fission yeast Rep2 is a putative transcriptional activator subunit for the cell cycle 'start' function of Res2-Cdc10. *EMBO J.*, **14**, 4794–4802.
- Baum, B., Wuari, J. and Nurse, P. (1997) Control of S-phase periodic transcription in the fission yeast mitotic cycle. *EMBO J.*, **16**, 4676–4688.
- Peng, X., Karuturi, R.K., Miller, L.D., Lin, K., Jia, Y., Kondu, P., Wang, L., Wong, L.S., Liu, E.T., Balasubramanian, M.K. et al. (2005) Identification of cell cycle-regulated genes in fission yeast. *Mol. Biol. Cell*, **16**, 1026–1042.
- Rustici, G., Mata, J., Kivinen, K., Lio, P., Penkett, C.J., Burns, G., Hayles, J., Brazma, A., Nurse, P. and Bahler, J. (2004) Periodic gene expression program of the fission yeast cell cycle. *Nat. Genet.*, **36**, 809–817.
- Aligianni, S., Lackner, D.H., Klier, S., Rustici, G., Wilhelm, B.T., Marguerat, S., Codlin, S., Brazma, A., de Bruin, R.A. and Bahler, J. (2009) The fission yeast homeodomain protein Yox1p binds to MBF and confines MBF-dependent cell-cycle transcription to G1-S via negative feedback. *PLoS Genet.*, **5**, e1000626.
- Fernandez Sarabia, M.J., McNerny, C., Harris, P., Gordon, C. and Fantes, P. (1993) The cell cycle genes *cdc22+* and *suc22+* of the fission yeast *Schizosaccharomyces pombe* encode the large and small subunits of ribonucleotide reductase. *Mol. Gen. Genet.*, **238**, 241–251.
- Connolly, T. and Beach, D. (1994) Interaction between the Cig1 and Cig2 B-type cyclins in the fission yeast cell cycle. *Mol. Cell Biol.*, **14**, 768–776.
- Hofmann, J.F. and Beach, D. (1994) *cdt1* is an essential target of the Cdc10/Sct1 transcription factor: requirement for DNA replication and inhibition of mitosis. *EMBO J.*, **13**, 425–434.
- Kelly, T.J., Martin, G.S., Forsburg, S.L., Stephen, R.J., Russo, A. and Nurse, P. (1993) The fission yeast *cdc18+* gene product couples S phase to START and mitosis. *Cell*, **74**, 371–382.
- Caetano, C., Klier, S. and de Bruin, R.A. (2011) Phosphorylation of the MBF repressor Yox1p by the DNA replication checkpoint keeps the G1/S cell-cycle transcriptional program active. *PLoS One*, **6**, e17211.
- Gómez-Escoda, B., Ivanova, T., Calvo, I.A., Alves-Rodrigues, I., Hidalgo, E. and Ayté, J. (2011) Yox1 links MBF-dependent transcription to completion of DNA synthesis. *EMBO Rep.*, **12**, 84–89.
- Ivanova, T., Gomez-Escoda, B., Hidalgo, E. and Ayte, J. (2011) G1/S transcription and the DNA synthesis checkpoint: common regulatory mechanisms. *Cell Cycle*, **10**, 912–915.
- Purtill, F.S., Whitehall, S.K., Williams, E.S., McNerny, C.J., Sharrocks, A.D. and Morgan, B.A. (2011) A homeodomain transcription factor regulates the DNA replication checkpoint in yeast. *Cell Cycle*, **10**, 664–670.
- Ayté, J., Schweitzer, C., Zarzov, P., Nurse, P. and DeCaprio, J.A. (2001) Feedback regulation of the MBF transcription factor by cyclin Cig2. *Nat. Cell Biol.*, **3**, 1043–1050.
- Zeman, M.K. and Cimprich, K.A. (2014) Causes and consequences of replication stress. *Nat. Cell Biol.*, **16**, 2–9.
- Ivanova, T., Alves-Rodrigues, I., Gomez-Escoda, B., Dutta, C., DeCaprio, J.A., Rhind, N., Hidalgo, E. and Ayte, J. (2013) The DNA damage and the DNA replication checkpoints converge at the MBF transcription factor. *Mol. Biol. Cell*, **24**, 3350–3357.
- Inoue, Y., Kitagawa, M. and Taya, Y. (2007) Phosphorylation of pRB at Ser612 by Chk1/2 leads to a complex between pRB and E2F-1 after DNA damage. *EMBO J.*, **26**, 2083–2093.
- Bertoli, C., Klier, S., McGowan, C., Wittenberg, C. and de Bruin, R.A. (2013) Chk1 inhibits E2F6 repressor function in response to replication stress to maintain cell-cycle transcription. *Curr. Biol.*, **23**, 1629–1637.
- Hartwell, L. (1992) Defects in a cell cycle checkpoint may be responsible for the genomic instability of cancer cells. *Cell*, **71**, 543–546.
- Lobrich, M. and Jeggo, P.A. (2007) The impact of a negligent G2/M checkpoint on genomic instability and cancer induction. *Nature Rev. Cancer*, **7**, 861–869.
- Li, B., Carey, M. and Workman, J.L. (2007) The role of chromatin during transcription. *Cell*, **128**, 707–719.
- Sterner, D.E. and Berger, S.L. (2000) Acetylation of histones and transcription-related factors. *Microbiol. Mol. Biol. Rev.*, **64**, 435–459.
- Kouzarides, T. (2007) Chromatin modifications and their function. *Cell*, **128**, 693–705.
- Bottomley, M.J. (2004) Structures of protein domains that create or recognize histone modifications. *EMBO Rep.*, **5**, 464–469.
- Nugent, R.L., Johnsson, A., Fleharty, B., Gogol, M., Xue-Franzen, Y., Seidel, C., Wright, A.P. and Forsburg, S.L. (2010) Expression profiling of *S. pombe* acetyltransferase mutants identifies redundant pathways of gene regulation. *BMC Genomics*, **11**, 59.
- Owen, D.J., Ornaghi, P., Yang, J.C., Lowe, N., Evans, P.R., Ballario, P., Neuhaus, D., Filetici, P. and Travers, A.A. (2000) The structural basis for the recognition of acetylated histone H4 by the bromodomain of histone acetyltransferase *gcn5p*. *EMBO J.*, **19**, 6141–6149.
- Li, S. and Shogren-Knaak, M.A. (2009) The Gcn5 bromodomain of the SAGA complex facilitates cooperative and cross-tail acetylation of nucleosomes. *J. Biol. Chem.*, **284**, 9411–9417.
- Helmlinger, D., Marguerat, S., Villen, J., Gygi, S.P., Bahler, J. and Winston, F. (2008) The *S. pombe* SAGA complex controls the switch from proliferation to sexual differentiation through the opposing roles of its subunits Gcn5 and Spt8. *Genes Dev.*, **22**, 3184–3195.
- Helmlinger, D. and Tora, L. (2017) Sharing the SAGA. *Trends Biochem. Sci.*, **42**, 850–861.
- Balasubramanian, R., Pray-Grant, M.G., Selleck, W., Grant, P.A. and Tan, S. (2002) Role of the Ada2 and Ada3 transcriptional coactivators in histone acetylation. *J. Biol. Chem.*, **277**, 7989–7995.
- Warfield, L., Ranish, J.A. and Hahn, S. (2004) Positive and negative functions of the SAGA complex mediated through interaction of Spt8 with TBP and the N-terminal domain of TFIIA. *Genes Dev.*, **18**, 1022–1034.
- Mohibullah, N. and Hahn, S. (2008) Site-specific cross-linking of TBP in vivo and in vitro reveals a direct functional interaction with the SAGA subunit Spt3. *Genes Dev.*, **22**, 2994–3006.



37. Govind,C.K., Zhang,F., Qiu,H., Hofmeyer,K. and Hinnebusch,A.G. (2007) Gcn5 promotes acetylation, eviction, and methylation of nucleosomes in transcribed coding regions. *Mol. Cell*, **25**, 31–42.
38. Sanso,M., Vargas-Perez,I., Quintales,L., Antequera,F., Ayte,J. and Hidalgo,E. (2011) Gcn5 facilitates Pol II progression, rather than recruitment to nucleosome-depleted stress promoters, in *Schizosaccharomyces pombe*. *Nucleic Acids Res.*, **39**, 6369–6379.
39. Wyce,A., Xiao,T., Whelan,K.A., Kosman,C., Walter,W., Eick,D., Hughes,T.R., Krogan,N.J., Strahl,B.D. and Berger,S.L. (2007) H2B ubiquitylation acts as a barrier to Ctk1 nucleosomal recruitment prior to removal by Ubp8 within a SAGA-related complex. *Mol. Cell*, **27**, 275–288.
40. Takahashi,Y., Rayman,J.B. and Dynlacht,B.D. (2000) Analysis of promoter binding by the E2F and pRB families in vivo: distinct E2F proteins mediate activation and repression. *Genes Dev.*, **14**, 804–816.
41. Lang,S.E., McMahon,S.B., Cole,M.D. and Hearing,P. (2001) E2F transcriptional activation requires TRRAP and GCN5 cofactors. *J. Biol. Chem.*, **276**, 32627–32634.
42. Bonnet,J., Wang,C.Y., Baptista,T., Vincent,S.D., Hsiao,W.C., Stierle,M., Kao,C.F., Tora,L. and Devys,D. (2014) The SAGA coactivator complex acts on the whole transcribed genome and is required for RNA polymerase II transcription. *Genes Dev.*, **28**, 1999–2012.
43. Taubert,S., Gorrini,C., Frank,S.R., Parisi,T., Fuchs,M., Chan,H.M., Livingston,D.M. and Amati,B. (2004) E2F-dependent histone acetylation and recruitment of the Tip60 acetyltransferase complex to chromatin in late G1. *Mol. Cell Biol.*, **24**, 4546–4556.
44. Martinez-Balbas,M.A., Bauer,U.M., Nielsen,S.J., Brehm,A. and Kouzarides,T. (2000) Regulation of E2F1 activity by acetylation. *EMBO J.*, **19**, 662–671.
45. Marzio,G., Wagener,C., Gutierrez,M.I., Cartwright,P., Helin,K. and Giacca,M. (2000) E2F family members are differentially regulated by reversible acetylation. *J. Biol. Chem.*, **275**, 10887–10892.
46. Chan,H.M., Krstic-Demonacos,M., Smith,L., Demonacos,C. and La Thangue,N.B. (2001) Acetylation control of the retinoblastoma tumour-suppressor protein. *Nat. Cell Biol.*, **3**, 667–674.
47. Nguyen,D.X., Baglia,L.A., Huang,S.M., Baker,C.M. and McCance,D.J. (2004) Acetylation regulates the differentiation-specific functions of the retinoblastoma protein. *EMBO J.*, **23**, 1609–1618.
48. Iyer,N.G., Xian,J., Chin,S.F., Bannister,A.J., Daigo,Y., Aparicio,S., Kouzarides,T. and Caldas,C. (2007) p300 is required for orderly G1/S transition in human cancer cells. *Oncogene*, **26**, 21–29.
49. Pickard,A., Wong,P.P. and McCance,D.J. (2010) Acetylation of Rb by PCAF is required for nuclear localization and keratinocyte differentiation. *J. Cell Sci.*, **123**, 3718–3726.
50. Moreno,S., Klar,A. and Nurse,P. (1991) Molecular genetic analysis of fission yeast *Schizosaccharomyces pombe*. *Meth. Enzymol.*, **194**, 795–823.
51. Bähler,J., Wu,J.Q., Longtine,M.S., Shah,N.G., McKenzie,A. 3rd, Steever,A.B., Wach,A., Philippsen,P. and Pringle,J.R. (1998) Heterologous modules for efficient and versatile PCR-based gene targeting in *Schizosaccharomyces pombe*. *Yeast*, **14**, 943–951.
52. Mellone,B.G., Ball,L., Suka,N., Grunstein,M.R., Partridge,J.F. and Allshire,R.C. (2003) Centromere silencing and function in fission yeast is governed by the amino terminus of histone H3. *Curr. Biol.*, **13**, 1748–1757.
53. Castillo,E.A., Vivancos,A.P., Jones,N., Ayte,J. and Hidalgo,E. (2003) *Schizosaccharomyces pombe* cells lacking the Ran-binding protein Hba1 show a multidrug resistance phenotype due to constitutive nuclear accumulation of Pap1. *J. Biol. Chem.*, **278**, 40565–40572.
54. Vivancos,A.P., Castillo,E.A., Biteau,B., Nicot,C., Ayte,J., Toledano,M.B. and Hidalgo,E. (2005) A cysteine-sulfenic acid in peroxiredoxin regulates H2O2-sensing by the antioxidant Pap1 pathway. *Proc. Natl. Acad. Sci. U.S.A.*, **102**, 8875–8880.
55. Calvo,I.A., Garcia,P., Ayte,J. and Hidalgo,E. (2012) The transcription factors Pap1 and Prr1 collaborate to activate antioxidant, but not drug tolerance, genes in response to H2O2. *Nucleic Acids Res.*, **40**, 4816–4824.
56. Moldon,A., Malapeira,J., Gabrielli,N., Gogol,M., Gomez-Escoda,B., Ivanova,T., Seidel,C. and Ayte,J. (2008) Promoter-driven splicing regulation in fission yeast. *Nature*, **455**, 997–1000.
57. Helmlinger,D., Marguerat,S., Villen,J., Swaney,D.L., Gygi,S.P., Bahler,J. and Winston,F. (2011) Tra1 has specific regulatory roles, rather than global functions, within the SAGA co-activator complex. *EMBO J.*, **30**, 2843–2852.
58. Tapia-Alveal,C., Lin,S.J., Yeoh,A., Jabado,O.J. and O'Connell,M.J. (2014) H2A.Z-dependent regulation of cohesin dynamics on chromosome arms. *Mol. Cell Biol.*, **34**, 2092–2104.
59. Xhemalce,B., Miller,K.M., Driscoll,R., Masumoto,H., Jackson,S.P., Kouzarides,T., Verreault,A. and Arcangoli,B. (2007) Regulation of histone H3 lysine 56 acetylation in *Schizosaccharomyces pombe*. *J. Biol. Chem.*, **282**, 15040–15047.
60. Wang,Y., Kallgren,S.P., Reddy,B.D., Kuntz,K., Lopez-Maury,L., Thompson,J., Watt,S., Ma,C., Hou,H., Shi,Y. *et al.* (2012) Histone H3 lysine 14 acetylation is required for activation of a DNA damage checkpoint in fission yeast. *J. Biol. Chem.*, **287**, 4386–4393.
61. Yang,H., Kwon,C.S., Choi,Y. and Lee,D. (2016) Both H4K20 mono-methylation and H3K56 acetylation mark transcription-dependent histone turnover in fission yeast. *Biochem Biophys Res. Com.*, **476**, 515–521.
62. Aoi,Y., Kawashima,S.A., Simanis,V., Yamamoto,M. and Sato,M. (2014) Optimization of the analogue-sensitive Cdc2/Cdk1 mutant by in vivo selection eliminates physiological limitations to its use in cell cycle analysis. *Open Biol.*, **4**, 140063.
63. Kim,H.S., Vanoosthuysen,V., Fillingham,J., Roguev,A., Watt,S., Kislinger,T., Treyer,A., Carpenter,L.R., Bennett,C.S., Emili,A. *et al.* (2009) An acetylated form of histone H2A.Z regulates chromosome architecture in *Schizosaccharomyces pombe*. *Nat. Struct. Mol. Biol.*, **16**, 1286–1293.
64. Knezevic,I., Gonzalez-Medina,A., Gaspa,L., Hidalgo,E. and Ayte,J. (2018) The INO80 complex activates the transcription of S-phase genes in a cell cycle-regulated manner. *FEBS J.*, **285**, 3870–3881.